NdhV Is a Subunit of NADPH Dehydrogenase Essential for Cyclic Electron Transport in *Synechocystis* sp. Strain PCC 6803[1]

Fudan Gao[2], Jiaohong Zhao[2], Xiaozhuo Wang, Shen Qin, Lanzhen Wei, and Weimin Ma*

College of Life and Environment Sciences, Shanghai Normal University, Shanghai 200234, China

ORCID IDs: 0000-0002-8882-5968 (F.G.); 0000-0003-4964-415X (W.M.).

Two mutants sensitive to heat stress for growth and impaired in NADPH dehydrogenase (NDH-1)-dependent cyclic electron transport around photosystem I (NDH-CET) were isolated from the cyanobacterium *Synechocystis* sp. strain PCC 6803 transformed with a transposon-bearing library. Both mutants had a tag in the same *sll0272* gene, encoding a protein highly homologous to NdhV identified in Arabidopsis (*Arabidopsis thaliana*). Deletion of the *sll0272* gene (*ndhV*) did not influence the assembly of NDH-1 complexes and the activities of CO_2 uptake and respiration but reduced the activity of NDH-CET. NdhV interacted with NdhS, a ferredoxin-binding subunit of cyanobacterial NDH-1 complex. Deletion of NdhS completely abolished NdhV, but deletion of NdhV had no effect on the amount of NdhS. Reduction of NDH-CET activity was more significant in Δ*ndhS* than in Δ*ndhV*. We therefore propose that NdhV cooperates with NdhS to accept electrons from reduced ferredoxin.

Cyanobacterial NADPH dehydrogenase (NDH-1) complexes are localized in the thylakoid membrane (Ohkawa et al., 2001, 2002; Zhang et al., 2004; Xu et al., 2008; Battchikova et al., 2011b) and participate in a variety of bioenergetic reactions, such as respiration, cyclic electron transport around photosystem I (NDH-CET), and CO_2 uptake (Ogawa, 1991; Mi et al., 1992; Ohkawa et al., 2000). Structurally, the cyanobacterial NDH-1 complexes closely resemble energy-converting complex I in eubacteria and the mitochondrial respiratory chain regardless of the absence of homologs of three subunits in cyanobacterial genomes that constitute the catalytically active core of complex I (Friedrich et al., 1995; Friedrich and Scheide, 2000; Arteni et al., 2006). Over the past decade, new subunits of NDH-1 complexes specific to oxygenic photosynthesis have been identified in several cyanobacterial strains. They are NdhM to NdhQ and NdhS (Prommeenate et al., 2004; Battchikova et al., 2005, 2011b; Nowaczyk et al., 2011; Wulfhorst et al., 2014; Zhang et al., 2014; Zhao et al., 2014b, 2015), in addition to NdhL first identified in the cyanobacterium *Synechocystis* sp. strain PCC 6803 (hereafter *Synechocystis* 6803) about 20 years ago (Ogawa, 1992). Among them, NdhS possesses a ferredoxin (Fd)-binding motif and was shown to bind Fd, which suggested that Fd is one of the electron donors to NDH-1 complexes (Mi et al., 1995; Battchikova et al., 2011b; Ma and Ogawa, 2015). Deletion of NdhS strongly reduced the activity of NDH-CET but had no effect on respiration and CO_2 uptake (Battchikova et al., 2011b; Ma and Ogawa, 2015). The NDH-CET plays an important role in coping with various environmental stresses regardless of its elusive mechanism. For example, this function can greatly alleviate heat-sensitive growth phenotypes (Wang et al., 2006a; Zhao et al., 2014a). Thus, heat treatment strategy can help in identifying the proteins essential to NDH-CET.

Here, a new oxygenic photosynthesis-specific (OPS) subunit NdhV was identified in *Synechocystis* 6803 with the help of heat treatment strategy, and its deletion did not influence the assembly of NDH-1L and NDH-1MS complexes and the activities of CO_2 uptake and respiration but impaired the NDH-CET activity. We give evidence that NdhV interacts with NdhS and is another component of Fd-binding domain of cyanobacterial NDH-1 complex. A possible role of NdhV on the NDH-CET activity is discussed.

RESULTS

Isolation of NDH-CET-Defective Mutants

The NDH-CET has a protective role against heat stress in cyanobacteria (Zhao et al., 2014a) and higher

[1] This work was supported by the National Natural Science Foundation of China (grant nos. 31370270 and 31570235) and the Shanghai Natural Science Foundation (grant no. 14ZR1430000).

[2] These authors contributed equally to the article.

* Address correspondence to wma@shnu.edu.cn.

The author responsible for distribution of materials integral to the findings presented in this article in accordance with the policy described in the Instructions for Authors (www.plantphysiol.org) is: Weimin Ma (wma@shnu.edu.cn).

W.M. designed and supervised the experiments; J.Z. performed the molecular and physiological experiments; F.G. performed the biochemical experiments; F.G., X.W., and S.Q. performed the protein-protein interaction experiments; F.G., J.Z., X.W., and S.Q. analyzed the data; L.W. and W.M. analyzed and interpreted the data; W.M. wrote the article.

www.plantphysiol.org/cgi/doi/10.1104/pp.15.01430

plants (Wang et al., 2006a). Under high temperature conditions, therefore, the growth of NDH-CET-defective mutants is markedly retarded compared with the wild type despite similar growth under growth temperature. To screen for NDH-CET-defective mutants, we transformed wild-type cells with a transposon-bearing library, thus tagging and inactivating many genes randomly, and then cultured the mutant cells under high temperature conditions. We isolated two mutants, which grew slowly in the 96-well plates under high temperature but grew similarly to the wild type under growth temperature (Fig. 1A).

To investigate whether the high temperature-sensitive growth phenotype of the two mutants resulted from defective NDH-CET, we monitored the postillumination rise in chlorophyll (Chl) fluorescence. This approach has been extensively used to monitor NDH-CET activity in cyanobacteria (Mi et al., 1995; Deng et al., 2003a; Ma and Mi, 2005; Battchikova et al., 2011b; Dai et al., 2013; Zhang et al., 2014; Zhao et al., 2014b, 2015) and higher plants (Burrows et al., 1998; Shikanai et al., 1998; Hashimoto et al., 2003; Wang et al., 2006b; Peng et al., 2009, 2011a, 2012; Sirpiö et al., 2009; Yamamoto et al., 2011; Armbruster et al., 2013). As shown in Figure 1B, the NDH-CET activity in both mutants was lower than that in the wild type as judged by the height and relative rate of postillumination increase in Chl fluorescence. The results indicate that NDH-CET is affected in mutants 1 and 2.

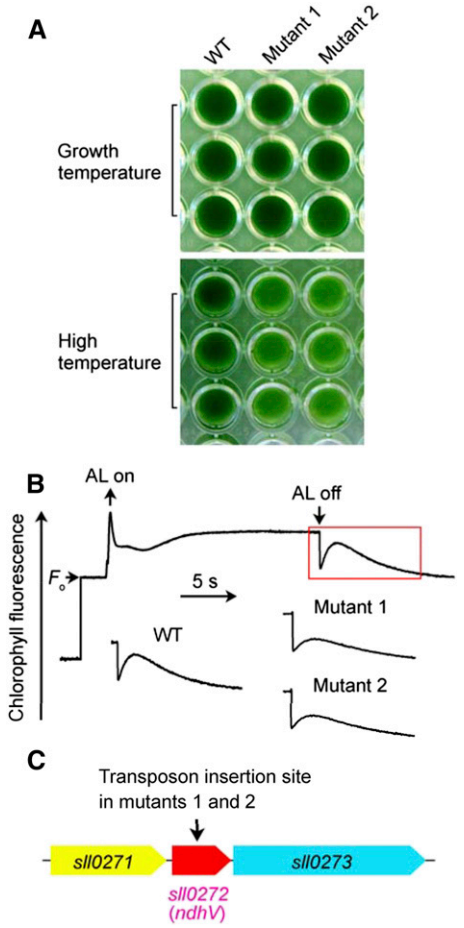

Figure 1. Use of heat condition to screen for NDH-CET-defective mutant in transposon-tagged mutant populations of *Synechocystis* 6803. A, Growth of the wild type (WT) and mutants under conditions of growth temperature (30°C) and high temperature (42°C). B, Monitoring of NDH-CET activity using Chl fluorescence analysis. The top curve shows a typical trace of Chl fluorescence in the wild-type *Synechocystis* 6803. Cells were exposed to AL (620 nm; 45 μmol photons m^{-2} s^{-1}) for 30 s. AL was turned off, and the subsequent change in the Chl fluorescence level was monitored as an indication of NDH-CET activity. C, The arrow schematically indicates the transposon insertion site in mutants 1 and 2 probed by PCR analysis using the primers listed in Supplemental Table S1.

To identify the genes inactivated by transposon tagging, we analyzed the sites of transposon insertion in both mutants. Sequencing analysis of the kanamycin resistance marker (Kam^R) insertion region revealed that both mutants were tagged in a gene, *sll0272* (Fig. 1C), at position 2104651 of the *Synechocystis* 6803 genome (NCBI-GI: 16331085; Kaneko et al., 1996). The gene encodes a highly hydrophilic protein (Supplemental Fig. S1) of 141 amino acids having an uncharacterized domain (DUF2996; Supplemental Fig. S2), which was highly homologous to NdhV (Supplemental Fig. S2) identified in Arabidopsis (*Arabidopsis thaliana*) using bioinformatic and reverse genetic approaches (Fan et al., 2015). This implies that inactivation of *ndhV* impairs NDH-CET activity.

Deletion of *ndhV* Impairs NDH-CET Activity

To confirm that inactivation of *ndhV* impairs NDH-CET activity, we replaced the majority of the *ndhV* coding region with a spectinomycin resistance marker (Sp^R; Fig. 2A). PCR analysis of the *ndhV* locus confirmed a complete segregation of the Δ*ndhV* mutant allele (Fig. 2B). Western analysis using an antibody specifically prepared against NdhV (see "Materials and Methods") demonstrated absence of the gene product in the mutant (Fig. 2C). As expected, the NDH-CET activity, as measured by the postillumination increase in Chl fluorescence, was lower in Δ*ndhV* than in the wild type. However, the activity remained relatively high compared with the M55 mutant (Fig. 2D). A similar result was obtained by measuring the oxidation of P700 by far-red (FR) light after actinic light (AL) illumination. When AL was turned off after 30-s illumination by AL (800 μmol photons m^{-2} s^{-1}) supplemented with FR light, $P700^+$ was transiently reduced by electrons from the plastoquinone pool, and subsequently P700 was reoxidized by background FR. Operation of the NDH-1 complexes, which transfer electrons from the reduced cytoplasmic pool to plastoquinone, hinders the reoxidation of P700 (Shikanai et al., 1998; Battchikova et al., 2011b; Dai et al., 2013; Zhang et al., 2014; Zhao et al., 2014b, 2015). The reoxidation of P700 was evidently faster in Δ*ndhV* compared with the wild type but was much slower than in M55

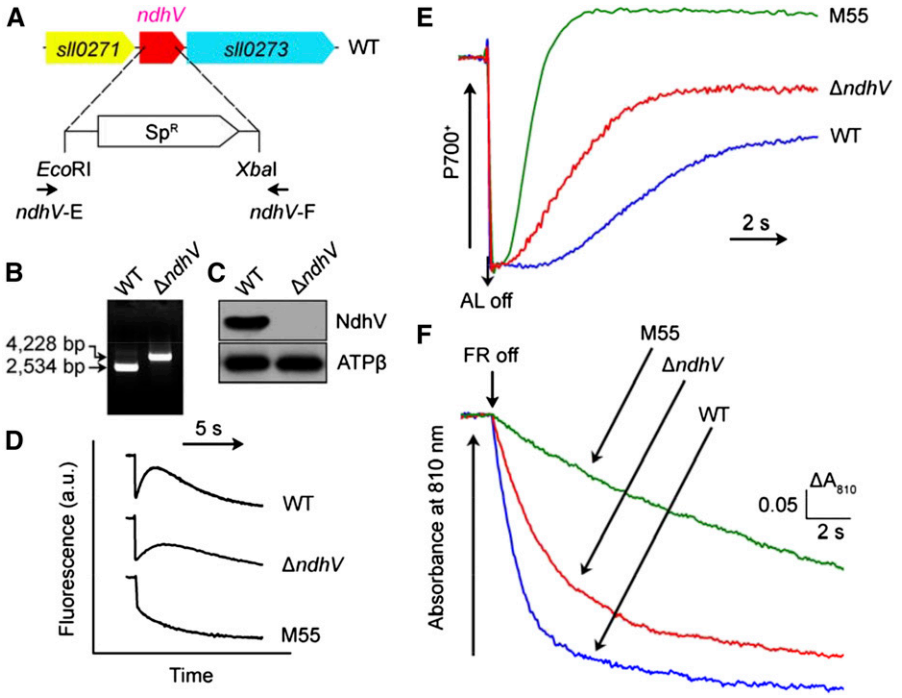

Figure 2. Deletion of *ndhV* gene and its effect on NDH-CET. A, Construction of plasmid used to generate *ndhV* inactivation mutant (Δ*ndhV*). B, PCR segregation analysis of the Δ*ndhV* mutant using the *ndhV*-E and *ndhV*-F primers (Supplemental Table S1). C, Western analysis of NdhV from total protein of the wild-type (WT) and Δ*ndhV* strains. Total protein corresponding to 1 μg Chl *a* was loaded onto each lane, and ATPβ was detected as a loading control. D, Monitoring of NDH-CET activity by Chl fluorescence. Experimental procedure as in Figure 1. a.u., Arbitrary units. E, Redox kinetics of P700 after termination of AL illumination (800 μmol photons m^{-2} s^{-1} for 30 s) under a background of FR light. The cells were illuminated by AL supplemented with FR light to store electrons in the cytoplasmic pool. After termination of AL illumination, $P700^+$ was transiently reduced by electrons from the plastoquinone pool; thereafter, P700 was reoxidized by background FR light. The redox kinetics of P700 were recorded. The $P700^+$ levels were standardized by their maximum levels attained by exposure to FR light. F, Kinetics of the $P700^+$ rereduction in darkness after turning off FR light in the presence of 10 μM DCMU. The Chl *a* concentration was adjusted to 20 μg mL^{-1} before measurement, and curves are normalized to the maximal signal.

(Fig. 2E). We also measured the NDH-CET by monitoring the reduction rate of $P700^+$ in darkness after illumination of cells with FR light. The rereduction of $P700^+$ was markedly slower in Δ*ndhV* compared with that in the wild type, although it was still faster than in M55 (Fig. 2F). Furthermore, the growth of Δ*ndhV* under heat stress conditions was evidently slower than the wild type despite similar growth under growth temperature (Supplemental Fig. S3). Taking these results together, we conclude that deletion of *ndhV* impairs the NDH-CET activity.

NdhV Has Similar Properties to NdhS

To reveal the function of NdhV further, we examined the effects of deletion of *ndhV* on the activities of CO_2 uptake and respiration. Deletion of *ndhV* did not have any effect on the growth of the mutant under either high or air level of CO_2 at pH 6.5 (Fig. 3). The deletion also did not influence the respiration activity (Fig. 4A) and the growth on plates with or without Glc and 3-(3,4-dichlorophenyl)-1,1-dimethylurea (DCMU; Fig. 4B). It is evident that the NdhV subunit is not involved in CO_2 uptake and respiration, regardless of the involvement of this subunit in NDH-CET.

To understand the function of NdhV, thylakoid membranes of the wild-type, Δ*ndhV*, and M55 strains grown under 2% (v/v) CO_2 (Fig. 5) and those of the wild-type and Δ*ndhV* strains grown under air (Supplemental Fig. S4) were subjected to blue native (BN)-PAGE. Deletion of *ndhV* did not influence the abundance of total NDH-1 (Fig. 5A), nor did it influence the assembly of NDH-1L and NDH-1MS complexes (Fig. 5, B and C; Supplemental Fig. S4, A–C), which are involved in respiration and CO_2 uptake, respectively (Zhang et al., 2004). This explains why NdhV does not participate in CO_2 uptake and respiration, although how deletion of *ndhV* impairs NDH-CET activity still remains elusive. However, we found that the roles of NdhV on the expression, assembly, and activity of NDH-1 complex are very similar to those of NdhS, a Fd-binding subunit of NDH-1 complex, as observed in this study (Figs. 3–5; Supplemental Fig. S4) and in the previous studies (Battchikova et al., 2011b; Ma and Ogawa, 2015). These similar properties of NdhV with NdhS

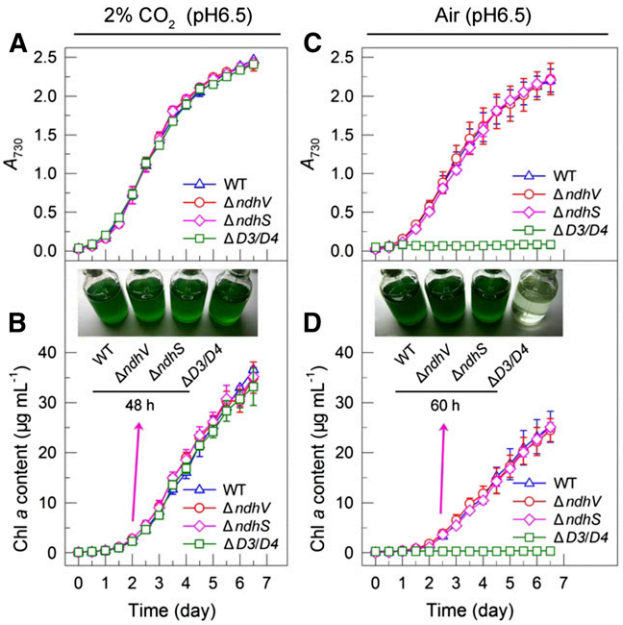

Figure 3. Growth of wild-type (WT), Δ*ndhV*, Δ*ndhS*, and Δ*D3/D4* cells. A and B, Cell density (A) and Chl *a* content (B) were monitored under 2% (v/v) CO_2 at pH 6.5. C and D, Cell density (C) and Chl *a* content (D) were monitored under air level of CO_2 at pH 6.5. Values are means ± SD ($n = 5$).

strongly suggest that NdhV may influence NDH-CET activity via NdhS.

NdhV Interacts with NdhS

To test this possibility, we determined the interaction of NdhV with NdhS by using a yeast two-hybrid system. The results clearly showed the interaction of NdhV with NdhS (Fig. 6A). The interaction was reinforced by the results of GST pull-down (Fig. 6, B and C). Therefore, we can conclude that NdhV interacts with NdhS, which greatly consolidated this possibility that NdhV is involved in NDH-CET via NdhS.

Stabilization of NdhV Requires NdhS

To obtain insights into how NdhV influenced NDH-CET via NdhS, we analyzed the amount of NdhV accumulated in the thylakoid membranes from the wild-type and Δ*ndhS* strains. Deletion of *ndhS* resulted in a complete absence of NdhV in the thylakoid membranes (Fig. 7A), but the deletion did not influence the transcript levels of *ndhV* (Supplemental Fig. S5). Conversely, deletion of *ndhV* did not influence the amount of NdhS in the thylakoid membranes (Fig. 7B). Based on the above results, we may conclude that NdhV is involved in stabilizing the binding of NdhS with reduced Fd in *Synechocystis* 6803 as schematically represented in Figure 8 and its absence destabilizes the binding, thereby impairing the NDH-CET activity.

DISCUSSION

Over the past decade, a significant achievement has been made in identifying the composition and function of OPS subunits from the NDH-1 complex in cyanobacteria (for review, see Battchikova and Aro, 2007; Ogawa and Mi, 2007; Ma, 2009; Battchikova et al., 2011a; Ma and Ogawa, 2015) and higher plants (for review, see Suorsa et al., 2009; Ifuku et al., 2011; Peng et al., 2011b). In this study, we newly identified an OPS subunit NdhV in the cyanobacterium *Synechocystis* 6803, which interacts with another OPS subunit NdhS having Fd-binding motif. Deletion of *ndhV* did not influence the abundance of total NDH-1, the assembly of NDH-1L and NDH-1MS complexes, and the activities of CO_2 uptake and respiration but reduced the NDH-CET activity, similar to the results of Δ*ndhS* mutant observed in this study and in previous studies (Battchikova et al., 2011b; Ma and Ogawa, 2015). These

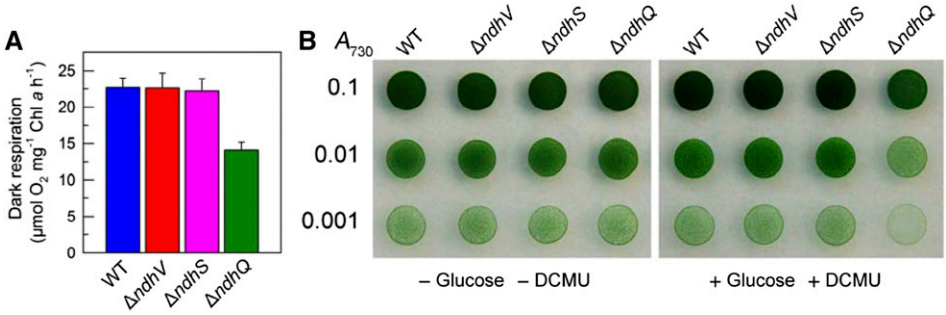

Figure 4. Respiration of wild-type (WT) and mutant cells. A, The rate of O_2 uptake in the dark at 30°C on wild-type, Δ*ndhV*, Δ*ndhS*, and Δ*ndhQ* cells grown under 2% (v/v) CO_2. The Chl *a* concentration was adjusted to 10 μg mL^{-1} before measurement. Bars indicate SES ($n = 5$). B, Growth of wild-type, Δ*ndhV*, Δ*ndhS*, and Δ*ndhQ* cells on agar plates in the absence (left) and presence (right) of Glc (5 mM) and DCMU (10 μM). Three microliters of cell suspensions with densities corresponding to A_{730} nm values of 0.1 (top rows), 0.01 (middle rows), and 0.001 (bottom rows) were spotted on agar plates and incubated under 2% (v/v) CO_2 in air for 6 d at 40 μmol photons m^{-2} s^{-1}.

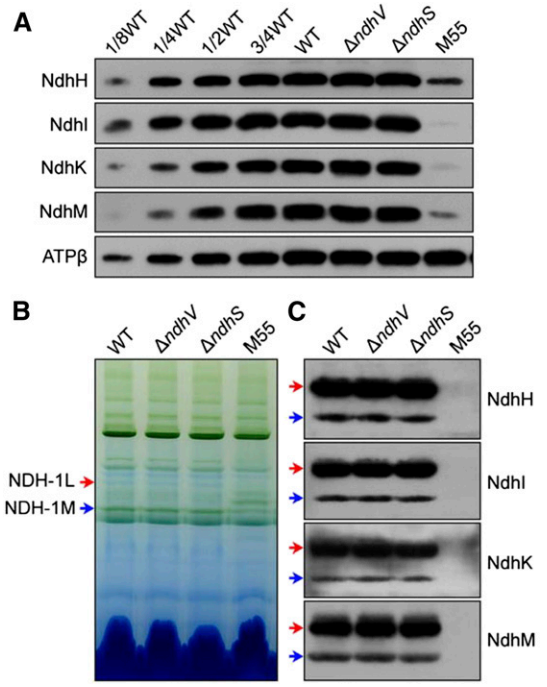

Figure 5. Western analyses of NDH-1L and NDH-1M complexes from the wild-type (WT), Δ*ndhV*, Δ*ndhS*, and M55 strains. A, Immunodetection of Ndh subunits in thylakoid membranes from the wild-type (including indicated serial dilutions), Δ*ndhV*, Δ*ndhS*, and M55 mutants. Immunoblotting was performed using antibodies against hydrophilic Ndh subunits (NdhH, NdhI, NdhK, and NdhM). Lanes were loaded with thylakoid membrane proteins corresponding to 1 μg Chl *a*. ATPβ was used as a loading control. B, Thylakoid protein complexes isolated from the wild type and mutants were separated by BN-PAGE. Thylakoid membrane extract corresponding to 9 μg Chl *a* was loaded onto each lane. Red and blue arrows indicate the positions of the NDH-1L and NDH-1M complexes, respectively. C, Protein complexes were electroblotted to a polyvinylidene difluoride membrane, and the membrane was cross-reacted with anti-NdhH, -NdhI, -NdhK, and -NdhM to probe the assembly of the NDH-1L and NDH-1M complexes.

similar properties of NdhV with NdhS and their interaction strongly suggested that just like NdhS, NdhV is also localized in Fd-binding domain of NDH-1 complex.

In higher plants, deletion of *ndhV* partially collapsed the assembly of hydrophilic arm and Fd-binding domains of chloroplast NDH-1, but no interaction was detected between NdhV and the subunits of these two domains (Fan et al., 2015). Thus, localization of NdhV in the chloroplast NDH-1 complex still remains elusive. By contrast, in cyanobacteria, deletion of *ndhV* did not influence the assembly of NDH-1L and NDH-1MS complexes, but NdhV interacts with NdhS in Fd-binding domain of NDH-1 complex. The results of this study further showed that deletion of *ndhS* completely abolished NdhV, but deletion of *ndhV* had no effect on the amount of NdhS. Together, these results strongly suggest that in Fd-binding domain of cyanobacterial NDH-1 complex, NdhV is localized at the surface of NdhS, as schematically represented in Figure 8. In addition, the topography of NdhV in cyanobacterial NDH-1 complex (see Fig. 8) suggests that NdhV may also interact directly with NdhI and/or NdhJ.

In higher plants, chloroplast NDH-1 complex was proposed to accept exclusively electrons from Fd, and NdhS was suggested to be a Fd-binding subunit of the complex based on the overall spatial homology of NdhS with the PsaE subunit of PSI complex (Yamamoto et al., 2011; Yamamoto and Shikanai, 2013). Because of a high homology of NdhS in cyanobacterial and chloroplastic NDH-1, cyanobacterial NdhS may also be a Fd-binding subunit of NDH-1 complex (Fig. 8). This possibility was supported by the interaction of NdhS with Fd (He et al., 2015). The results of this study further suggested that NdhV may be essential to stabilize the binding of NdhS with Fd based on the following reasons: (1) NdhV interacts with NdhS; (2) deletion of *ndhV* had no effect on the amount of NdhS, but the deletion reduced the NDH-CET activity; and (3) reduction of NDH-CET activity was more significant in Δ*ndhS* than in Δ*ndhV* as deduced from the results of this study and a previous study (Battchikova et al., 2011b). We therefore propose that in cyanobacteria, NdhV cooperates with NdhS to form a functional structure of Fd-binding domain included in NDH-1 complex, as schematically represented in Figure 8.

In higher plants, NdhT and NdhU were proposed to localize in Fd-binding domain of chloroplast NDH-1 complex and were suggested to cooperate with NdhS to accept electrons from reduced Fd (Yamamoto et al., 2011;

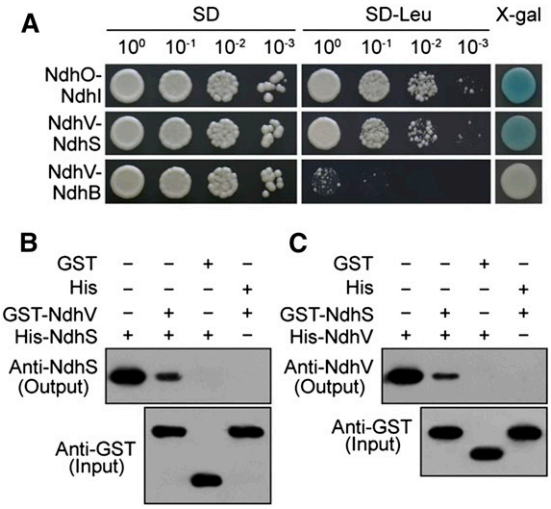

Figure 6. Interaction of NdhV with NdhS. A, NdhV and NdhS were separately constructed into bait and prey vectors and transformed into the yeast strain EGY48. Transformed yeast was diluted and dropped onto SD media, Leu-negative (−Leu) SD media, or X-gal media. The interactions of NdhO-NdhI and NdhV-NdhB were assayed as positive and negative controls, respectively. B and C, The expressed proteins were mixed and incubated with GST beads on a rotating shaker at 4°C overnight. After washing, the interactions of GST-NdhV with His-NdhS (B) and GST-NdhS with His-NdhV (C) were detected using the antibodies against NdhS and NdhV, respectively. The interactions of GST (without NdhV or NdhS) with His-NdhS or His-NdhV and of pET32a vector backbone with GST-NdhV or GST-NdhS were used as negative controls.

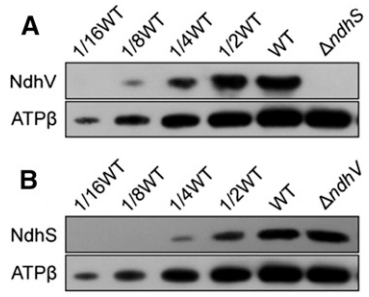

Figure 7. Stabilization of NdhV requires NdhS but not vice versa. Western analysis of NdhV subunit from the wild type (WT; including indicated serial dilutions) and Δ*ndhS* (A) or of NdhS subunit from the wild type and Δ*ndhV* (B). Lanes were loaded with thylakoid membrane proteins corresponding to 1 μg Chl *a*. ATPβ was used as a loading control.

Yamamoto and Shikanai, 2013). However, the counterparts of NdhT and NdhU are absent in cyanobacteria. Therefore, it appears plausible that except NdhV and NdhS, new OPS subunits, not yet identified, also exist in Fd-binding domain structure of cyanobacterial NDH-1 complex.

In addition to Fd, NADPH has suggested to be another electron donor to NDH-1 in cyanobacteria (Mi et al., 1995; Matsuo et al., 1998; Deng et al., 2003a, 2003b; Ma et al., 2006; Ma and Mi, 2008; Hu et al., 2013; Ma and Ogawa, 2015). Electron donation from Fd to NDH-1 may contribute mainly to NDH-CET and NADPH may donate principally to CO_2 uptake and respiration, since deletion of NdhV or NdhS significantly impaired NDH-CET but did not influence CO_2 uptake and respiration as indicated by the results of this study and previous studies (Battchikova et al., 2011b; Ma and Ogawa, 2015). Consequently, it is possible that deletion of other new members of Fd-binding domain structure of cyanobacterial NDH-1 complex except NdhV and NdhS, not yet identified, also impaired NDH-CET significantly but had no effect on CO_2 uptake and respiration.

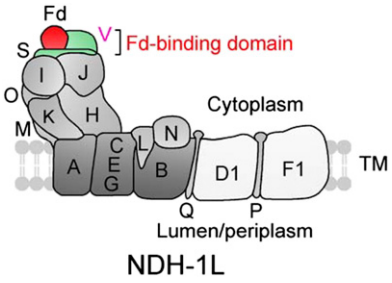

Figure 8. A model schematically represents the localization of NdhV in Fd-binding domain of cyanobacterial NDH-1 complex. NdhV, which was suggested to be located at the surface of NdhS, may stabilize the binding of NdhS with reduced Fd in Fd-binding domain of cyanobacterial NDH-1 complex. NdhS and NdhV are two OPS subunits and are indicated by green. TM, Thylakoid membrane.

MATERIALS AND METHODS

Culture Conditions

Glc-tolerant strain of wild-type *Synechocystis* 6803 and its mutants, Δ*ndhS* (Battchikova et al., 2011b), Δ*ndhV*, Δ*ndhB* (M55; Ogawa, 1991), Δ*ndhD3/D4* (Δ*D3/D4*; Ohkawa et al., 2000), and Δ*ndhQ* (Zhao et al., 2015), were cultured at 30°C or 42°C in BG-11 medium (Allen, 1968) buffered with either Tris-HCl (5 mM, pH 8.0) or MES-KOH (20 mM, pH 6.5) by bubbling with 2% (v/v) CO_2 in air or air alone. Solid medium was BG-11 supplemented with 1.5% (w/v) agar. The mutant strains were grown in the presence of appropriate antibiotics under illumination by fluorescence lamps at 40 μmol photons m^{-2} s^{-1}.

Isolation and Construction of Mutants

A cosmid library of *Synechocystis* 6803 genome was constructed. The library that contained 10^5 clones with inserts of 35 to 38.5 kb was subjected to in vitro transposon mutagenesis using EZ-Tn5 < KAN-2 > Insertion Kit (Epicentre Biotechnologies) and then used to transform the wild-type cells of *Synechocystis* 6803. Following transformation, cells were spread on 1.5% (w/v) BG-11 agar plates supplemented with 5 μg mL^{-1} kanamycin, and Kam^R mutants that grew slowly under heat stress conditions but normally under growth temperature were isolated. Genomic DNA isolated from each mutant was digested with *Hha*I and after self-ligation was used as a template for inverse PCR with primers (Supplemental Table S1) complementary to the N- and C-terminal regions of the Kam^R cassette. The exact position of the cassette in the mutant genome was determined by sequencing the PCR product.

The *ndhV* gene with flanking sequences was amplified by PCR using primers *ndhV*-A and -B (Supplemental Table S1) and was ligated into the *pEASY*-Blunt Zero vector (TransGen Biotech) to generate *pEASY*-Blunt Zero-*ndhV* plasmid. A DNA fragment encoding spectinomycin resistance (Sp^R) cassette was also amplified by PCR creating *Eco*RI and *Xba*I sites using primers *ndhV*-C and -D (Supplemental Table S1) and was inserted into the *ndhV* gene at *Xba*I and *Eco*RI sites to generate the *pEASY*-Blunt Zero-Δ*ndhV* plasmid (Fig. 2A), which was used to transform the wild-type cells to generate the Δ*ndhV* mutant. The transformants were spread on agar plates containing BG-11 medium and spectinomycin (10 μg mL^{-1}) buffered at pH 8.0, and the plates were incubated in 2% (v/v) CO_2 in air under illumination by fluorescent lamps at 40 μmol photons m^{-2} s^{-1} (Williams and Szalay, 1983; Long et al., 2011). The mutated *ndhV* in the transformants was segregated to homogeneity (by successive-streak purification) as determined by PCR amplification and western analysis (Fig. 2, B and C).

Chl Fluorescence and P700 Analysis

The transient increase in Chl fluorescence after actinic light had been turned off was monitored as described (Ma and Mi, 2005). The redox kinetics of P700 was measured according to previously described methods (Battchikova et al., 2011b; Dai et al., 2013; Zhang et al., 2014; Zhao et al., 2014b, 2015). The rereduction of $P700^+$ in darkness was measured with a Dual-PAM-100 (Walz) with an emitter-detector unit ED-101US/MD by monitoring absorbance changes at 830 nm and using 875 nm as a reference. Cells were kept in the dark for 2 min and 10 μM DCMU was added to the cultures prior to the measurement. The P700 was oxidized by FR light with a maximum at 720 nm from LED lamp for 30 s, and the subsequent rereduction of $P700^+$ in the dark was monitored.

Growth Curve

The cell density of wild-type, Δ*ndhV*, Δ*ndhS*, and Δ*D3/D4* cells cultured under pH 6.5 and 2% (v/v) CO_2 in air or air alone was determined every 12 h by measuring the A_{730} nm using a spectrophotometer (UV3000; Shimadzu).

Wild-type, Δ*ndhV*, Δ*ndhS*, and Δ*D3/D4* cells (1.5 mL) were collected by centrifugation, and pigments in the pellet were extracted by 1.5 mL methyl alcohol. Chl *a* in the extract was determined using a spectrophotometer (UV3000; Shimadzu) and was calculated according to the formula: Chl *a* (μg mL^{-1}) = 13.9 × A_{665} (Arnon, 1949).

Dark Respiration

Oxygen uptake was measured at 30°C (Hansatech) with a Clark-type oxygen electrode according to the method of Ma and Mi (2005). Cells were suspended in fresh BG-11 medium at a Chl *a* concentration of 10 μg mL^{-1}.

Isolation of Crude Thylakoid Membranes

The cell cultures (5 L) were harvested at the logarithmic phase (A_{730} = 0.6–0.8) and washed twice by 50 mL of fresh BG-11 medium and then thylakoid membranes were isolated according to Gombos et al. (1994) with some modifications as follows. Cells were suspended in 5 mL of disruption buffer (10 mM HEPES-NaOH, 5 mM sodium phosphate, pH 7.5, 10 mM $MgCl_2$, 10 mM NaCl, and 25% [v/v] glycerol) and after adding zirconia/silica beads, broken by vortexing 20 times at the highest speed for 30 s at 4°C with 5 min cooling on ice between the runs. The crude extract was centrifuged at 5,000*g* for 5 min to remove the glass beads and unbroken cells. By further centrifugation at 20,000*g* for 30 min, we obtained crude thylakoid membranes from the precipitation.

Electrophoresis and Immunoblotting

BN-PAGE of *Synechocystis* 6803 membranes was performed as described previously (Kügler et al., 1997) with slight modifications (Battchikova et al., 2011b; Dai et al., 2013; Zhang et al., 2014; Zhao et al., 2014b, 2015). Isolated membranes were prepared for BN-PAGE as follows. Membranes were washed with 330 mM sorbitol, 50 mM Bis-Tris, pH 7.0, and 0.5 mM phenylmethylsulfonyl fluoride (Sigma), and resuspended in 20% (w/v) glycerol, 25 mM Bis-Tris, pH 7.0, 10 mM $MgCl_2$, 0.1 units RNase-free DNase RQ1 (Promega) at a Chl *a* concentration of 0.3 mg mL^{-1}, and 0.5 mM phenylmethylsulfonyl fluoride. The samples were incubated on ice for 10 min, and an equal volume of 3% (w/v) *n*-dodecyl-β-D-maltoside was added. Solubilization was performed for 40 min on ice. Insoluble components were removed by centrifugation at 18,000*g* for 15 min. The collected supernatant was mixed with 1/10 volume of sample buffer, 5% (w/v) Serva Blue G, 100 mM Bis-Tris, pH 7.0, 30% (w/v) Suc, 500 mM ε-amino-*n*-caproic acid, and 10 mM EDTA. Solubilized membranes were then applied to a 0.75-mm-thick, 5% to 12.5% (w/v) acrylamide gradient gel (Hoefer Mighty Small mini-vertical unit). Samples were loaded on an equal Chl *a* basis per lane. Electrophoresis was performed at 4°C by increasing the voltage gradually from 50 V up to 200 V during the 5.5-h run.

SDS-PAGE of *Synechocystis* 6803 crude thylakoid membranes was carried out on 12% (w/v) polyacrylamide gel with 6 M urea as described earlier (Laemmli, 1970).

For immunoblotting, the proteins were electrotransferred to a polyvinylidene difluoride membrane (Immobilon-P; Millipore) and detected by protein-specific antibodies using an ECL assay kit (Amersham Pharmacia) according to the manufacturer's protocol. Antibody against NdhV subunit (the Sll0272 protein) of *Synechocystis* 6803 was raised in our laboratory. To amplify the *sll0272* gene, primer sequences were designed and are listed in Supplemental Table S1. The PCR products were ligated into vector pET32a, and the construct was amplified in *Escherichia coli* DH-5*α*. The plasmid was used to transform *E. coli* strain BL21(DE3)pLysS for expression. The gene expression products from *E. coli* were purified and used as antigens to immunize rabbits to produce polyclonal antibodies. Antibodies against NdhH, NdhI, NdhK, NdhM, NdhS, and ATPβ proteins of *Synechocystis* 6803 were previously raised in our laboratory (Ma and Mi, 2005; Battchikova et al., 2011b; Zhao et al., 2014b). Antibody against GST was purchased from Shanghai Immune Biotech, and antibody against NdhD3 was provided from Professor Eva-Mari Aro (Department of Biochemistry, University of Turku).

Yeast Two-Hybridization

Yeast two-hybridization was performed using a LexA system (Clontech). The PCR-amplified gene fragment of *ndhO* or *ndhV* was cloned in frame into *Eco*RI and *Xho*I or *Xho*I sites of pLexA, respectively, to form the bait construct (primers are shown in Supplemental Table S1). The fragments containing *ndhB*, *ndhI*, and *ndhS* genes were amplified by PCR, and inserted into either *Xho*I or *Eco*RI and *Xho*I sites of pJG4-5 to form the prey construct (primers are shown in Supplemental Table S1). The bait and prey constructs together with a reporter vector pSH18-34 were cotransformed into yeast strain EGY48 according to the manufacturer's instructions for the Matchmaker LexA two-hybrid system (Clontech). Transformed yeast was diluted and dropped onto synthetic dropout (SD) medium, Leu-negative (−Leu) SD medium, or X-gal medium, then grown at 30°C in darkness as described previously (Sun et al., 2009; Dai et al., 2013).

Expression and Purification of Fusion Proteins

The target proteins NdhV and NdhS were fused to different tags as follows. (1) The fragments containing *ndhV* and *ndhS* genes were amplified by PCR, and inserted between *Bam*HI and *Sac*I or *Bam*HI and *Eco*RI sites of pET32a, respectively, to form the His-tagged fusion protein constructs (primers are shown in Supplemental Table S1). (2) PCR-amplified *ndhV* or *ndhS* gene was cloned correspondingly in-frame into *Xho*I or *Eco*RI and *Xho*I sites of pGEX-5X-1 to form the GST-tagged fusion protein constructs (primers are shown in Supplemental Table S1). Subsequently, these constructs were transformed into *E. coli* strain BL21(DE3)pLysS and induced by 1 mM isopropyl-β-D-thiogalactoside for 16 h at 16°C to express His- and GST-tagged fusion proteins. These fusion proteins were purified at 4°C using Ni column (GE Healthcare) and glutathione Sepharose 4B (GE Healthcare), respectively, according to the manufacturer's instructions.

GST Pull-Down Assay

The GST pull-down assay was performed as described previously (Zhao et al., 2014b) with some modifications. To test the interaction of NdhV with NdhS, an equal amount of GST and GST-NdhV or GST-NdhS was separately incubated with 20 μL of glutathione Sepharose 4B beads (GE Healthcare) in 300 μL of binding buffer (50 mM Tris-HCl, pH 7.4, 100 mM NaCl, 5 mM EDTA, 0.5% [v/v] Triton X-100, 1 mM phenylmethanesulfonyl fluoride, and 1 mM DTT) at 4°C for 1 h. The beads were washed three times with 1 mL of binding buffer, and then an equal amount of His and His-NdhS or His-NdhV was separately added and incubated in a 300-μL reaction system on a rotating shaker at 4°C overnight. After the overnight incubation, the beads were pelleted by centrifugation and washed four times with the ice-cold binding buffer described above. The washed pellets were resuspended in 30 μL of 1× SDS (2% [w/v]) loading buffer and then boiled for 5 min. After centrifugation, the supernatant was collected and subjected to immunoblotting analysis.

RNA Extraction and Reverse Transcription PCR Analysis

Total RNA was isolated and analyzed as described previously (McGinn et al., 2003). Reverse transcription PCR (RT-PCR) was performed using the Access RT-PCR system (Promega) to generate products corresponding to *ndhV* and *16 S rRNA*, with 0.5 μg of DNase-treated total RNA as starting material. RT-PCR conditions were 95°C for 5 min, followed by cycles of 95°C, 62°C, and 72°C for 30 s each. The reactions were stopped after 20 or 30 cycles for *16 S rRNA* and after 30 or 40 cycles for *ndhV*. The primers used are summarized in Supplemental Table S1.

Sequence data from this article can be found in the GenBank/EMBL data libraries under accession numbers Sll0272 (NP_441813.1) and Ssl0352 (NP_442353.1).

Supplemental Data

The following supplemental materials are available.

Supplemental Figure S1. Prediction of transmembrane region for Sll0272.

Supplemental Figure S2. Sequence comparison between Sll0272 (*Synechocystis* 6803) and NdhV (Arabidopsis; At2g04039).

Supplemental Figure S3. Growth of wild-type and Δ*ndhV* cells under different temperature conditions.

Supplemental Figure S4. Western analyses of NDH-1 complexes from the air-grown wild-type, Δ*ndhV*, and Δ*ndhS* cells.

Supplemental Figure S5. RT-PCR analysis of *ndhV* in the wild-type and Δ*ndhS* strains.

Supplemental Table S1. Primers used in this study.

ACKNOWLEDGMENTS

We thank Professor Teruo Ogawa (Nagoya University) for reading the manuscript with critical comments and Professor Eva-Mari Aro (University of Turku) for the NdhD3 antibody.

Received September 9, 2015; accepted December 1, 2015; published December 7, 2015.

LITERATURE CITED

Allen MM (1968) Simple conditions for growth of unicellular blue-green algae on plates. J Phycol **4:** 1–4

Armbruster U, Rühle T, Kreller R, Strotbek C, Zühlke J, Tadini L, Blunder T, Hertle AP, Qi Y, Rengstl B, et al (2013) The photosynthesis affected mutant68-like protein evolved from a PSII assembly factor to mediate assembly of the chloroplast NAD(P)H dehydrogenase complex in Arabidopsis. Plant Cell **25:** 3926–3943

Arnon DI (1949) Copper enzymes in isolated chloroplasts. Polyphenoloxidase in *Beta valgaris.* Plant Physiol **24:** 1–15

Arteni AA, Zhang P, Battchikova N, Ogawa T, Aro EM, Boekema EJ (2006) Structural characterization of NDH-1 complexes of *Thermosynechococcus elongatus* by single particle electron microscopy. Biochim Biophys Acta **1757:** 1469–1475

Battchikova N, Aro EM (2007) Cyanobacterial NDH-1 complexes: multiplicity in function and subunit composition. Physiol Plant **131:** 22–32

Battchikova N, Eisenhut M, Aro EM (2011a) Cyanobacterial NDH-1 complexes: novel insights and remaining puzzles. Biochim Biophys Acta **1807:** 935–944

Battchikova N, Wei L, Du L, Bersanini L, Aro EM, Ma W (2011b) Identification of novel Ssl0352 protein (NdhS), essential for efficient operation of cyclic electron transport around photosystem I, in NADPH:plastoquinone oxidoreductase (NDH-1) complexes of *Synechocystis* sp. PCC 6803. J Biol Chem **286:** 36992–37001

Battchikova N, Zhang P, Rudd S, Ogawa T, Aro EM (2005) Identification of NdhL and Ssl1690 (NdhO) in NDH-1L and NDH-1M complexes of *Synechocystis* sp. PCC 6803. J Biol Chem **280:** 2587–2595

Burrows PA, Sazanov LA, Svab Z, Maliga P, Nixon PJ (1998) Identification of a functional respiratory complex in chloroplasts through analysis of tobacco mutants containing disrupted plastid *ndh* genes. EMBO J **17:** 868–876

Dai H, Zhang L, Zhang J, Mi H, Ogawa T, Ma W (2013) Identification of a cyanobacterial CRR6 protein, Slr1097, required for efficient assembly of NDH-1 complexes in *Synechocystis* sp. PCC 6803. Plant J **75:** 858–866

Deng Y, Ye J, Mi H (2003a) Effects of low CO_2 on NAD(P)H dehydrogenase, a mediator of cyclic electron transport around photosystem I in the cyanobacterium *Synechocystis* PCC6803. Plant Cell Physiol **44:** 534–540

Deng Y, Ye JY, Mi HL, Shen YG (2003b) [Separation of hydrophobic NAD(P)H dehydrogenase subcomplexes from cyanobacterium *Synechocystis* PCC6803]. Sheng Wu Hua Xue Yu Sheng Wu Wu Li Xue Bao (Shanghai) **35:** 723–727

Fan X, Zhang J, Li W, Peng L (2015) The NdhV subunit is required to stabilize the chloroplast NADH dehydrogenase-like complex in Arabidopsis. Plant J **82:** 221–231

Friedrich T, Scheide D (2000) The respiratory complex I of bacteria, archaea and eukarya and its module common with membrane-bound multisubunit hydrogenases. FEBS Lett **479:** 1–5

Friedrich T, Steinmüller K, Weiss H (1995) The proton-pumping respiratory complex I of bacteria and mitochondria and its homologue in chloroplasts. FEBS Lett **367:** 107–111

Gombos Z, Wada H, Murata N (1994) The recovery of photosynthesis from low-temperature photoinhibition is accelerated by the unsaturation of membrane lipids: a mechanism of chilling tolerance. Proc Natl Acad Sci USA **91:** 8787–8791

Hashimoto M, Endo T, Peltier G, Tasaka M, Shikanai T (2003) A nucleus-encoded factor, CRR2, is essential for the expression of chloroplast *ndhB* in Arabidopsis. Plant J **36:** 541–549

He Z, Zheng F, Wu Y, Li Q, Lv J, Fu P, Mi H (2015) NDH-1L interacts with ferredoxin via the subunit NdhS in *Thermosynechococcus elongatus.* Photosynth Res **126:** 341–349

Hu P, Lv J, Fu P, Hualing M (2013) Enzymatic characterization of an active NDH complex from *Thermosynechococcus elongatus.* FEBS Lett **587:** 2340–2345

Ifuku K, Endo T, Shikanai T, Aro EM (2011) Structure of the chloroplast NADH dehydrogenase-like complex: nomenclature for nuclear-encoded subunits. Plant Cell Physiol **52:** 1560–1568

Kaneko T, Sato S, Kotani H, Tanaka A, Asamizu E, Nakamura Y, Miyajima N, Hirosawa M, Sugiura M, Sasamoto S, et al (1996) Sequence analysis of the genome of the unicellular cyanobacterium *Synechocystis* sp. strain PCC6803. II. Sequence determination of the entire genome and assignment of potential protein-coding regions. DNA Res **3:** 109–136

Kügler M, Jänsch L, Kruft V, Schmitz UK, Braun HP (1997) Analysis of the chloroplast protein complexes by blue-native polyacrylamide gel electrophoresis (BN-PAGE). Photosynth Res **53:** 35–44

Laemmli UK (1970) Cleavage of structural proteins during the assembly of the head of bacteriophage T4. Nature **227:** 680–685

Long Z, Zhao J, Zhang J, Wei L, Wang Q, Ma W (2011) Effects of different light treatments on the natural transformation of *Synechocystis* sp. strain PCC 6803. Afr J Microbiol Res **5:** 3603–3610

Ma W (2009) Identification, regulation and physiological functions of multiple NADPH dehydrogenase complexes in cyanobacteria. Front Biol China **4:** 137–142

Ma W, Deng Y, Ogawa T, Mi H (2006) Active NDH-1 complexes from the cyanobacterium *Synechocystis* sp. strain PCC 6803. Plant Cell Physiol **47:** 1432–1436

Ma W, Mi H (2005) Expression and activity of type 1 NAD(P)H dehydrogenase at different growth phases of the cyanobacterium, *Synechocystis* PCC6803. Physiol Plant **125:** 135–140

Ma W, Mi H (2008) Effect of exogenous glucose on the expression and activity of NADPH dehydrogenase complexes in the cyanobacterium *Synechocystis* sp. strain PCC 6803. Plant Physiol Biochem **46:** 775–779

Ma W, Ogawa T (2015) Oxygenic photosynthesis-specific subunits of cyanobacterial NADPH dehydrogenases. IUBMB Life **67:** 3–8

Matsuo M, Endo T, Asada K (1998) Properties of the respiratory NAD(P)H dehydrogenase isolated from the cyanobacterium *Synechocystis* PCC6803. Plant Cell Physiol **39:** 263–267

McGinn PJ, Price GD, Maleszka R, Badger MR (2003) Inorganic carbon limitation and light control the expression of transcripts related to the CO_2-concentrating mechanism in the cyanobacterium *Synechocystis* sp. strain PCC6803. Plant Physiol **132:** 218–229

Mi H, Endo T, Ogawa T, Asada K (1995) Thylakoid membrane-bound, NADPH-specific pyridine nucleotide dehydrogenase complex mediated cyclic electron transport in the cyanobacterium *Synechocystis* sp. PCC 6803. Plant Cell Physiol **36:** 661–668

Mi H, Endo T, Schreiber U, Ogawa T, Asada K (1992) Electron donation from cyclic and respiratory flows to the photosynthetic intersystem chain is mediated by pyridine nucleotide dehydrogenase in the cyanobacterium *Synechocystis* PCC 6803. Plant Cell Physiol **33:** 1233–1237

Nowaczyk MM, Wulfhorst H, Ryan CM, Souda P, Zhang H, Cramer WA, Whitelegge JP (2011) NdhP and NdhQ: two novel small subunits of the cyanobacterial NDH-1 complex. Biochemistry **50:** 1121–1124

Ogawa T (1991) A gene homologous to the subunit-2 gene of NADH dehydrogenase is essential to inorganic carbon transport of *Synechocystis* PCC6803. Proc Natl Acad Sci USA **88:** 4275–4279

Ogawa T (1992) Identification and characterization of the *ictA/ndhL* gene product essential to inorganic carbon transport of *Synechocystis* PCC6803. Plant Physiol **99:** 1604–1608

Ogawa T, Mi H (2007) Cyanobacterial NADPH dehydrogenase complexes. Photosynth Res **93:** 69–77

Ohkawa H, Pakrasi HB, Ogawa T (2000) Two types of functionally distinct NAD(P)H dehydrogenases in *Synechocystis* sp. strain PCC6803. J Biol Chem **275:** 31630–31634

Ohkawa H, Sonoda M, Hagino N, Shibata M, Pakrasi HB, Ogawa T (2002) Functionally distinct NAD(P)H dehydrogenases and their membrane localization in *Synechocystis* sp. PCC6803. Funct Plant Biol **29:** 195–200

Ohkawa H, Sonoda M, Shibata M, Ogawa T (2001) Localization of NAD(P)H dehydrogenase in the cyanobacterium *Synechocystis* sp. strain PCC 6803. J Bacteriol **183:** 4938–4939

Peng L, Fukao Y, Fujiwara M, Shikanai T (2012) Multistep assembly of chloroplast NADH dehydrogenase-like subcomplex A requires several nucleus-encoded proteins, including CRR41 and CRR42, in Arabidopsis. Plant Cell **24:** 202–214

Peng L, Fukao Y, Fujiwara M, Takami T, Shikanai T (2009) Efficient operation of NAD(P)H dehydrogenase requires supercomplex formation with photosystem I via minor LHCI in Arabidopsis. Plant Cell **21:** 3623–3640

Peng L, Fukao Y, Myouga F, Motohashi R, Shinozaki K, Shikanai T (2011a) A chaperonin subunit with unique structures is essential for folding of a specific substrate. PLoS Biol **9:** e1001040

Peng L, Yamamoto H, Shikanai T (2011b) Structure and biogenesis of the chloroplast NAD(P)H dehydrogenase complex. Biochim Biophys Acta **1807:** 945–953

Prommeenate P, Lennon AM, Markert C, Hippler M, Nixon PJ (2004) Subunit composition of NDH-1 complexes of *Synechocystis* sp. PCC 6803: identification of two new *ndh* gene products with nuclear-encoded homologues in the chloroplast Ndh complex. J Biol Chem **279:** 28165–28173

Shikanai T, Endo T, Hashimoto T, Yamada Y, Asada K, Yokota A (1998) Directed disruption of the tobacco *ndhB* gene impairs cyclic electron flow around photosystem I. Proc Natl Acad Sci USA **95:** 9705–9709

Sirpiö S, Allahverdiyeva Y, Holmström M, Khrouchtchova A, Haldrup A, Battchikova N, Aro EM (2009) Novel nuclear-encoded subunits of the chloroplast NAD(P)H dehydrogenase complex. J Biol Chem **284:** 905–912

Sun SY, Chao DY, Li XM, Shi M, Gao JP, Zhu MZ, Yang HQ, Luan S, Lin HX (2009) OsHAL3 mediates a new pathway in the light-regulated growth of rice. Nat Cell Biol **11:** 845–851

Suorsa M, Sirpiö S, Aro EM (2009) Towards characterization of the chloroplast NAD(P)H dehydrogenase complex. Mol Plant **2:** 1127–1140

Wang P, Duan W, Takabayashi A, Endo T, Shikanai T, Ye JY, Mi H (2006b) Chloroplastic NAD(P)H dehydrogenase in tobacco leaves functions in alleviation of oxidative damage caused by temperature stress. Plant Physiol **141:** 465–474

Wang P, Ye J, Shen Y, Mi H (2006a) The role of chloroplast NAD(P)H dehydrogenase in protection of tobacco plant against heat stress. Sci China C Life Sci **49:** 311–321

Williams JGK, Szalay AA (1983) Stable integration of foreign DNA into the chromosome of the cyanobacterium *Synechococcus* R2. Gene **24:** 37–51

Wulfhorst H, Franken LE, Wessinghage T, Boekema EJ, Nowaczyk MM (2014) The 5 kDa protein NdhP is essential for stable NDH-1L assembly in *Thermosynechococcus elongatus.* PLoS One **9:** e103584

Xu M, Ogawa T, Pakrasi HB, Mi H (2008) Identification and localization of the CupB protein involved in constitutive CO_2 uptake in the cyanobacterium, *Synechocystis* sp. strain PCC 6803. Plant Cell Physiol **49:** 994–997

Yamamoto H, Peng L, Fukao Y, Shikanai T (2011) An Src homology 3 domain-like fold protein forms a ferredoxin binding site for the chloroplast NADH dehydrogenase-like complex in Arabidopsis. Plant Cell **23:** 1480–1493

Yamamoto H, Shikanai T (2013) In planta mutagenesis of Src homology 3 domain-like fold of NdhS, a ferredoxin-binding subunit of the chloroplast NADH dehydrogenase-like complex in Arabidopsis: a conserved Arg-193 plays a critical role in ferredoxin binding. J Biol Chem **288:** 36328–36337

Zhang J, Gao F, Zhao J, Ogawa T, Wang Q, Ma W (2014) NdhP is an exclusive subunit of large complex of NADPH dehydrogenase essential to stabilize the complex in *Synechocystis* sp. strain PCC 6803. J Biol Chem **289:** 18770–18781

Zhang P, Battchikova N, Jansen T, Appel J, Ogawa T, Aro EM (2004) Expression and functional roles of the two distinct NDH-1 complexes and the carbon acquisition complex NdhD3/NdhF3/CupA/Sll1735 in *Synechocystis* sp PCC 6803. Plant Cell **16:** 3326–3340

Zhao J, Gao F, Qiu Z, Wang Q, Ma W (2014a) Deletion of an electron donor-binding subunit of the NDH-1 complex, NdhS, results in a heat-sensitive growth phenotype in *Synechocystis* sp. PCC 6803. Chin Sci Bull **59:** 4484–4490

Zhao J, Gao F, Zhang J, Ogawa T, Ma W (2014b) NdhO, a subunit of NADPH dehydrogenase, destabilizes medium size complex of the enzyme in *Synechocystis* sp. strain PCC 6803. J Biol Chem **289:** 26669–26676

Zhao J, Rong W, Gao F, Ogawa T, Ma W (2015) Subunit Q is required to stabilize the large complex of NADPH dehydrogenase in *Synechocystis* sp. strain PCC 6803. Plant Physiol **168:** 443–451